Journal of Biomimetics, Biomaterials & Tissue Engineering Vol. 19 (2014) pp 87-98
Online available since 2014/Mar/24 at www.scientific.net

doi:10.4028/www.scientific.net/JBBTE.19.87

Damping Micromechanisms for Bones Above Room Temperature

Osvaldo A. Lambri[1, a *], José I. Pérez-Landazábal[2,b], Federico G. Bonifacich[1,c], Vicente Recarte[2,d], Melania L. Lambri[1,e], Griselda I. Zelada[1,f], Federico Tarditti[1,g], Damián Gargicevich[1,h]

[1]Laboratorio de Materiales, Escuela de Ingeniería Eléctrica, Centro de Tecnología e Investigación Eléctrica, Facultad de Ciencias Exactas, Ingeniería y Agrimensura, Universidad Nacional de Rosario – CONICET, Avda. Pellegrini 250, 2000 Rosario, Argentina.

[2]Departamento de Física, Universidad Pública de Navarra, Campus de Arrosadía s/n, 31006 Pamplona, Spain

[a]olambri@fceia.unr.edu.ar, [b]ipzlanda@unavarra.es, [c]bonifaci@fceia.unr.edu.ar, [d]recarte@unavarra.es, [e]melania.lambri@gmail.com, [f]gizelada@fceia.unr.edu.ar, [g]tarditti@fceia.unr.edu.ar, [h]gargi@fceia.unr.edu.ar

Keywords: Bone, Mechanical Spectroscopy, Differential Scanning Calorimetry, Thermogravimetry, Scanning Electron Microscopy

Abstract. The wide damping maximum which is reported to appear in bones, involving both cortical and cancellous parts, between around 280 K and 420 K; has been determined to be a composition of different processes taking place at different temperatures in cancellous and cortical parts. In fact, in the present work the mechanical response of cow ribs bones has been analysed by coupling mechanical spectroscopy, differential scanning calorimetry, thermogravimetry and scanning electron microscopy studies. Cancellous part develops two damping maxima at around 320 K and 350 K. Cortical part exhibits a wide maximum in damping between around 310 K and 410 K and another damping relaxation between 390 K and 410 K. The physical-chemical driving force giving rise to the above relaxation processes are discussed.

Introduction

Bone is a hierarchical composite material including up to seven levels of organisation. In the smallest level, bones are composed of carbonated apatite (dahllite) which is inserted or dispersed between the oriented type I collagen fibrils [1 – 5]. The outstanding mechanical properties of bones are not only related to their main components. The mesostructure and/or nanostructure play an important role in both the superior stiffness and the strength properties found in bones. Indeed, the composition alone does not fully explain the bulk mechanical properties. Mechanical properties in bones can vary significantly as a result of differences in the arrangement of their structure, testing direction (anisotropy) and anatomical location [3 – 7].

Mechanical spectroscopy (MS, also called dynamic mechanical analysis) is very sensitive to the microstructure of the sample and usually involves the simultaneous measurement of the damping (internal friction or loss tangent, $\tan(\phi)$) and the natural oscillating frequency, f, (f^2 being proportional to the elastic modulus) as a function of temperature [8, 9]. The knowledge of the driving force which controls the damping and the dynamic modulus behaviour should help to improve the prosthesis characteristics and so the life quality of persons either having orthopaedic prosthesis or suffering some disease as for instance osteoporosis. Several works about the dynamic-mechanical behaviour of bones have been reported in the literature, e.g. see Refs. [3 – 5, 10] and cited papers therein.

In general, bones show a wide damping peak in the 300 K – 380 K temperature range at strains within the physiological ranges (10^{-4} - 10^{-3}). This peak was observed both in chicken [4] and in cow [5] samples. Nevertheless, the physical and chemical processes which control the damping and modulus behaviour in this temperature range are still unclear.

In the present work, different techniques like MS, Differential Scanning Calorimetry (DSC), Thermogravimetry (TGA) and Scanning Electron Microscopy (SEM) were simultaneously applied on bones samples obtained from ribs of fresh cow meat. The correlation between the different techniques allows us to determine the physical and chemical mechanisms which are involved in the damping response within the temperature range 280 K - 420 K. Therefore, this work should contribute to the research fields on the orthopaedic, the novel bone replacements and also the osteoporosis.

Experimental

Samples. Studied bones were ribs of fresh cow meat purchased from three different providers. Samples were taken from bones by cutting with a jeweller saw in perpendicular direction to its longest dimension, as it is shown in Fig. 1. Different sample types were used: Samples including both the cortical and cancellous parts (a-type), samples made of cancellous bone part only (b-type) and samples made of cortical bone part only (c-type), see Fig. 1. The first type of samples will be called also hereafter composite-type samples. Three samples of each type were prepared from the bones of each provider. Parallelepiped shaped samples of around 3 mm x 4 mm x 40 mm, 3 mm x 11 mm x 30 mm and 3 mm x 3 mm x 15 mm, were used for each type, respectively. The final size for the samples was reached by means of mechanical polishing.

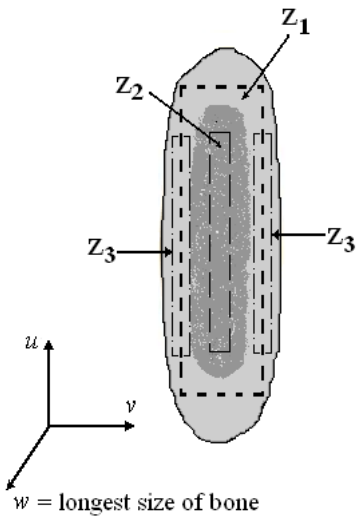

Figure 1. Schematic representation of a section of a rib bone obtained by cutting with the jeweller saw. Z1: Zone delimited by short dashed lines from where the composite-type sample was obtained. Z2: Zone delimited by long dashed lines from where the cancellous sample was obtained. Z3: Zones delimited by alt-dashed lines from where the cortical samples were obtained.

Measurements. MS studies were performed at different frequencies (f) close to 1.5 Hz and 15 Hz, as a function of temperature, T. The dynamical response of a linear viscoelastic material is usually described in terms of the complex modulus G* (or complex compliance J*) as a function of the circular frequency ω ($\omega=2\cdot\pi\cdot f$) and T. The complex modulus is generally presented in terms of its real and imaginary parts, that is, G* = G' + i G'', where G´ is the storage modulus, G'' is the loss modulus and i is the imaginary unit. Consequently, tan(ϕ) is defined as the quotient between the imaginary and real part of the complex modulus [8, 9, 11, 12]. In addition, a proportionality between G' and the squared natural oscillating frequency can be established. The proportionality constant involves the moment of inertia of the oscillating system and the dimensions of the sample [10, 13, 14].

MS measurements were performed in torsion under pure argon at atmospheric pressure [15]. The heating and cooling rates were 1K/min. A heating and its corresponding cooling run will be called

hereafter a thermal cycle [16, 17]. The maximum shear strain on the sample was 2 x 10^{-4} which is within the physiological range. The error for tan(ϕ) and f^2 was less than 4%.

It should be mentioned that MS measurements can exhibit differences between samples of the same type, but the results showed in this work represent the general trends of the whole set of studied samples. The measured values of damping and dynamic modulus, between samples taken from different ribs, exhibited usually a bandwidth of discrepancy around 10%, but in some cases we have also found a bandwidth up to around 20%. Nevertheless, the general trends of the curves during the thermal cycles are completely similar and reproducible. Moreover, we can assert that samples prepared from the same fresh ribs-bone at the same time and measured within two days of difference after storage in the refrigerator exhibit negligible differences.

DSC measurements at a heating/cooling rate of 10 K/min were carried out in a TA Q100 DSC equipment under nitrogen atmosphere. The weight loss (TGA, BOECO balance with a precision of 0.1 mg) was determined after a heating/cooling process at 2K/min up to different maximum temperatures, T_m, in argon atmosphere. The weight loss was determined as $\rho = (\omega_i - \omega(T_m))/\omega_i$, where ω_i is the initial weight at room temperature (RT) and $\omega(T_m)$ is the weight measured at RT after a cycle reaching a maximum T_m temperature. The error in the measured points was less than 0.02%.

A SEM Jeol (JSM-5610LV) was employed to characterise at RT the morphology and structure of the samples. Secondary electron images were obtained working at 20 kV. The specimens were coated with 5 nm of Silver.

Results and Discussion

Fig. 2(a) shows the damping (tan(ϕ)) for a composite-type sample (a-type) measured during the first thermal cycle, at 1.5 Hz, from 250 K up to 410 K. Damping exhibits two peaks at around 320 K and at 350 K during the heating run (full symbols). Besides, below RT the peak at around 270 K can be related to the melting of ice both of water and fluids located at the bone cavities and channels [4]. The next cooling measurement shows a reduction in the damping values, but a small peak at 350 K can be still identified (see empty symbols). Fig. 2(b) shows the corresponding squared natural oscillating frequency evolution. Frequency curve exhibits a decrease during the first heating run, up to around 320K followed by an increase, as temperature increases. In contrast, frequency increases during the cooling run markedly. The decrease in f^2 from around 270 K up to 320 K can be related to the melting of the ice both of water and fluids. In fact, the ice particles are inclusions harder than the matrix, so their appearance lead to an increase in the modulus of the sample and vice-versa [6, 13, 14, 16, 18 – 22]. Therefore, as it can be inferred from Fig. 2, both the damping and the squared resonance frequency show a clear hysteretic behaviour between heating and cooling curves. The hysteretic behaviour reduces as soon as successive thermal cycles are performed in a similar way to previous reported works [5, 23].

Fig. 3 shows the damping response measured at 15 Hz (circles) and at 1.5 Hz (squared triangles) for a-type samples. Both damping peaks are overlaid within the temperature range 300 K – 400 K (see inset) indicating that the mechanisms involved in the processes are not thermally activated, i.e., the relaxation does not shift in temperature as the oscillation frequency is modified [8, 9]. Fig. 3 also shows the damping curve measured at 15 Hz (diamonds in the Figure) corresponding to a composite-type sample with a high water amount. This sample exhibits a large damping peak related to the melting of iced water and fluids at around 273 K. In fact, a larger content of water leads to a higher peak at 273 K since the larger modification in the internal stresses into the matrix during the freezing or melting processes [6, 13, 14, 18, 22, 24, 25]. In addition, the larger is the peak related to the water, the larger are the damping values within the temperature interval 280 K – 360 K. Nevertheless, above 360 K, independently of both the water content and the oscillating frequency, all the damping spectra overlap.

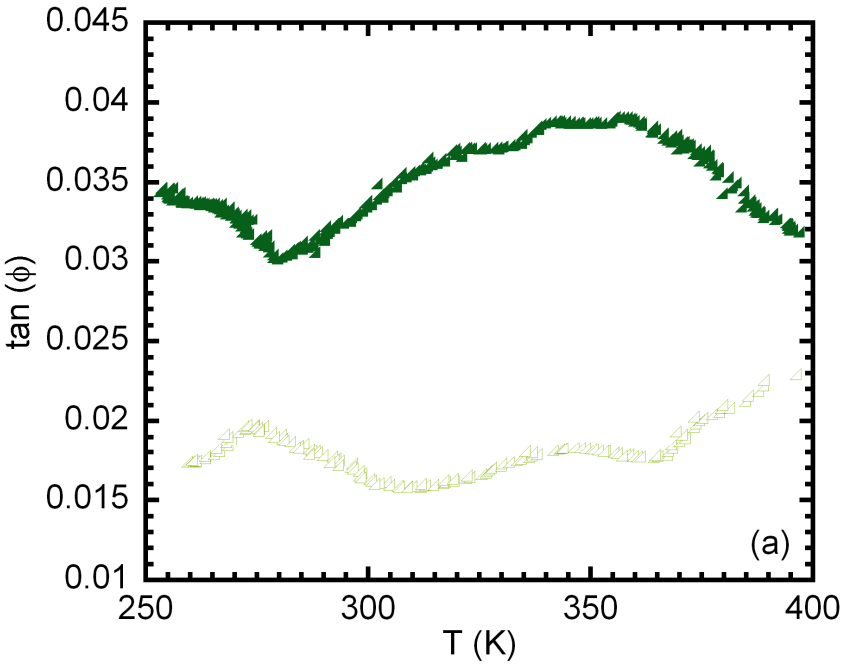

Figure 2(a). tan(ϕ) as a function of temperature during the first thermal cycle measured at around 1.5 Hz for a composite-type sample. Full squared-triangles: first heating. Empty squared-triangles: first cooling.

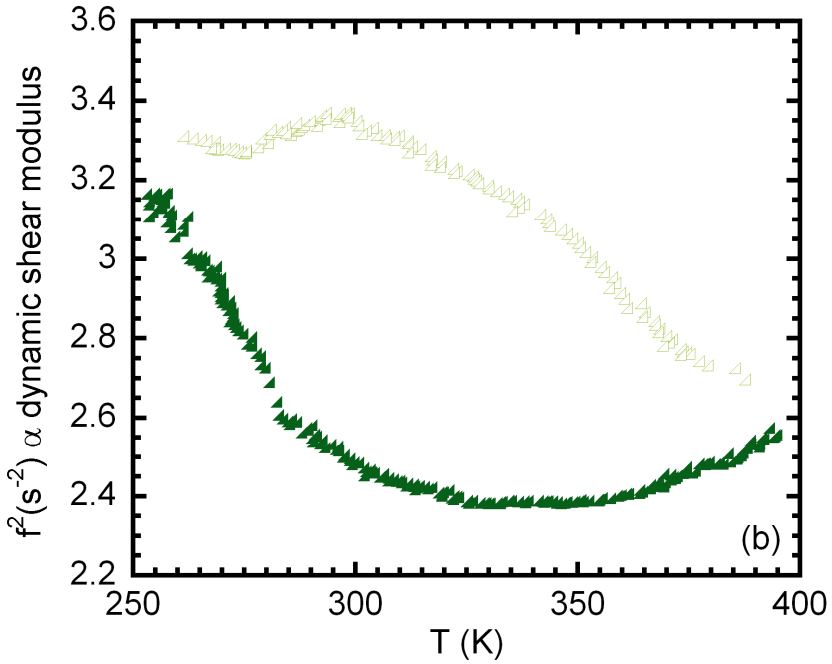

Figure 2(b). Dynamic shear modulus as a function of temperature during the first thermal cycle corresponding to data from Fig. 2(a). Symbols mean as in Fig. 2(a).

The two-peak contribution to the damping within the temperature interval 320 K - 380 K, for the composite-type sample with high water content, cannot be distinguished due to the background contribution from the water.

Besides, a sample taken from the same bone giving the spectrum plotted by means of full diamonds in Fig. 3, was dehydrated under vacuum of around 80 mTorr during 36 hours. This sample shows smaller damping values below 360 K, see empty diamonds in Fig. 3, and so, the loss of fluids and water lead to a decrease in damping. Indeed, a larger content of fluids and water makes easier the viscous movement of the dissipative micromechanisms leading to an increase in the mechanical energy losses [8, 9], i.e. water and fluids play the role of the plasticisers in polymers [26].

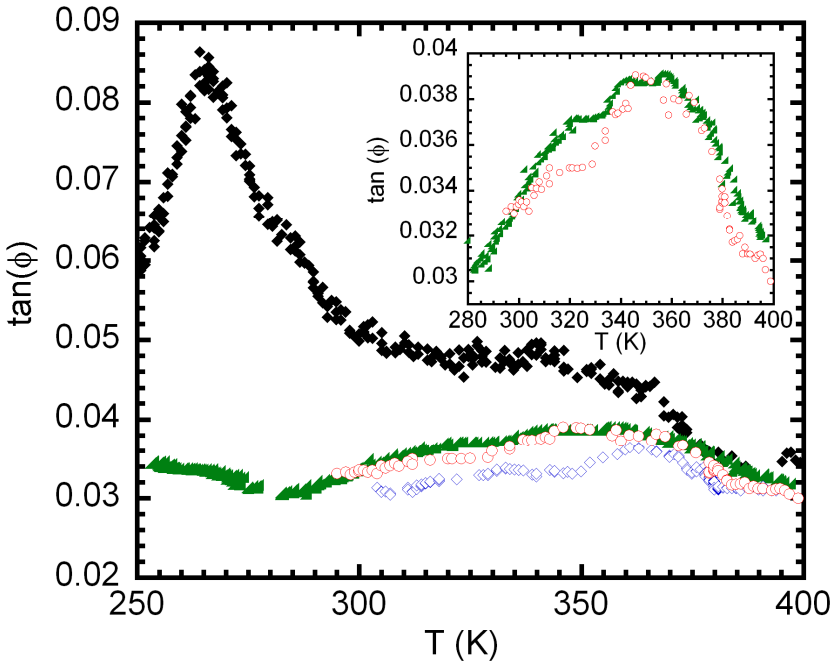

Figure 3. tan(ϕ) as a function of temperature for different samples measured at different oscillating frequencies. Squared-triangles correspond to the first heating curve from Fig. 2(a) (low frequency). Circles correspond to the first heating measured at high frequency for a composite-type sample. Full diamonds correspond to a sample with higher water content, measured at high frequency. Empty diamonds correspond to a dehydrated sample (see explanation in the text). Inset: Zoom for tan(ϕ) values between 0.028 and 0.04 for the first heating in composite-type samples measured at low and high frequencies.

Therefore, it is clearly revealed that both damping maxima, within the temperature interval 280 K – 400 K, are not thermally activated. In addition, the water and fluids content are involved in these relaxation processes.

With the aim of recognising the physical and chemical mechanisms which give rise to the relaxation peaks at around 320 K and 350 K, each bone part during the MS tests was measured independently. Fig. 4(a) shows the damping curves measured during heating on cancellous (b-type sample, triangles), cortical ((c) sample, inverted triangles) and a composite-type sample (a-type, circles), at 15 Hz. In addition, Fig. 4(b) shows the squared frequency curves corresponding to the damping spectra shown in Fig. 4(a). Cancellous samples show two clear maxima at around 320 K and 350 K, triangles in Fig. 4(a). In contrast, for cortical samples, the damping shows a wide peak between around 300 K and 400 K, see inverted triangles in Fig. 4(a). The damping spectrum corresponding to the composite sample (a) is also shown in this Figure to make clearer the comparison among of spectra (see circles). As it can be seen from Fig. 4(a), the damping curve for a composite-type sample (a) shows a behaviour that can be considered the superposition of the two component parts.

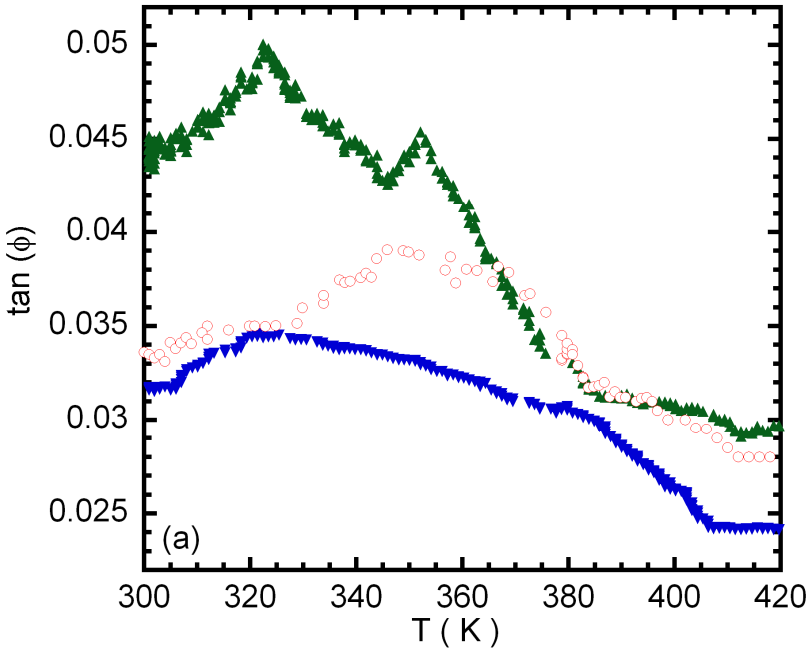

Figure 4(a). tan(ϕ) as a function of temperature during the first heating measured at around 15 Hz for different samples. Circles: composite-type sample. Triangles: Cancellous sample (b). Inverted triangles: Cortical sample (c).

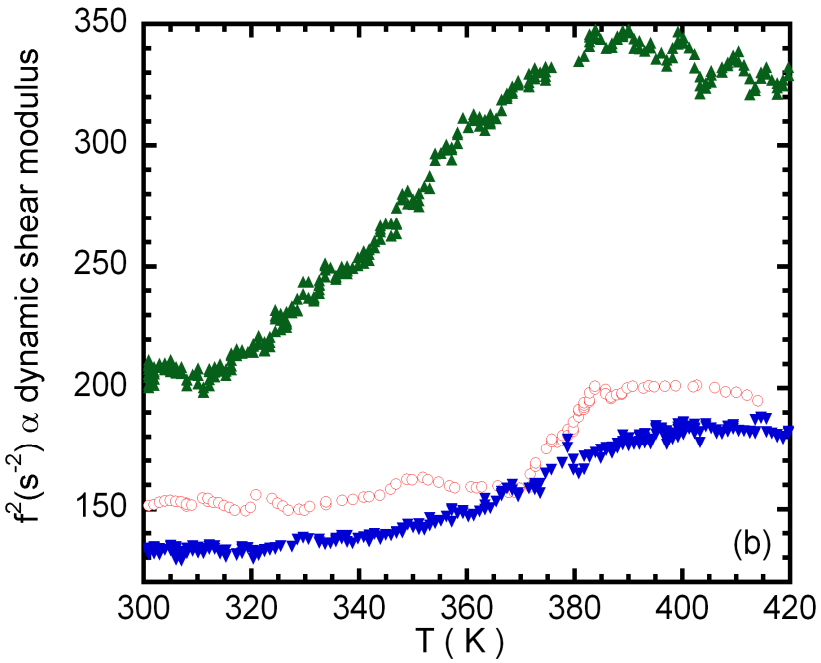

Figure 4(b). Dynamic shear modulus as a function of temperature during the first heating corresponding to data from Fig. 4(a). Symbols mean as in Fig. 4(a).

In order to know the different physical and chemical processes taking place during heating, the bones were studied by means of DSC and TGA measurements. DSC thermograms for cancellous (b) and cortical (c) samples are shown in Fig. 5. Focusing first on cancellous bone, the water amount was determined by comparing the enthalpy of the endothermic peak P_1 at 273 K with the melting enthalpy of water (ΔH_m=334 J/g), see Table 1. A mass of water of around 5% in cancellous bone was estimated. Two more endothermic peaks can be observed at around 320 K (P_2) and 373 K (P_3) during heating. P_2 peak could be related to the denaturation of albumin, and haemoglobin proteins [27] but also to the melting of fats [28]. On the other side, P_3 peak at 373 K can be related to the

vaporization of water. In fact, around 5% of mass of water has been estimated again taking into account the vaporization enthalpy of water (ΔH_v=2260 J/g) and the measured enthalpy of P_3 peak, Table 1.

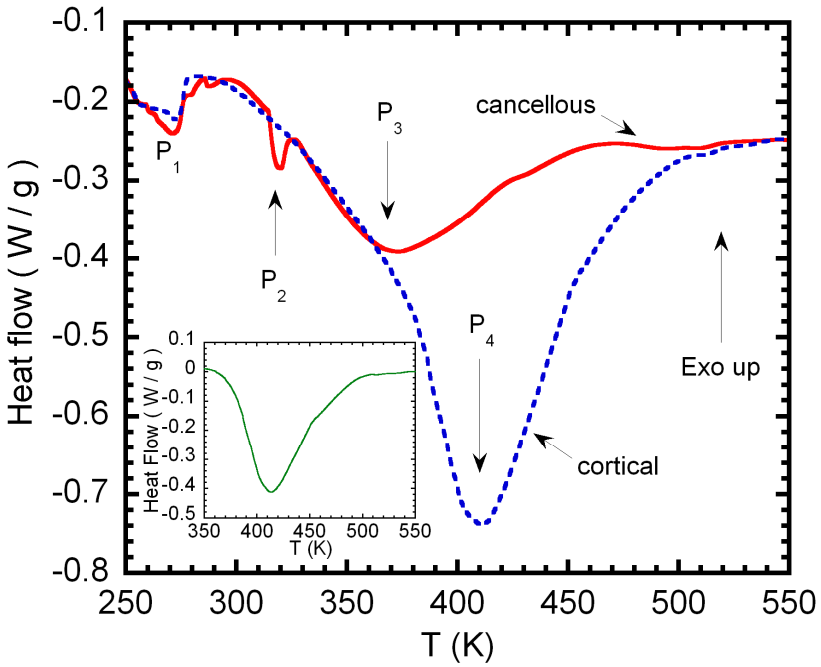

Figure 5. DSC thermograms measured during heating for cancellous bone (b sample) and cortical bone (c sample). Inset: Curve for cortical bone after subtraction of P_3, see explanation in the text.

Table 1. Temperature and enthalpies of the different peaks observed in the DSC thermograms in Fig. 5.

	Cancellous part		Cortical part	
Peak	***T*(K)**	***Q*(J/g)**	***T*(K)**	***Q*(J/g)**
P1	273	16	273	16
P2	320	2.4	-	-
P3	373	100	373	100
P4	-	-	410	160

The cortical bone (c sample) did not show P_2 peak clearly, but both the P_1 and P_3 peaks related to the water were similar. Nevertheless, a slight hump within the temperature range related to P_2 peak in cortical samples could be arising (Fig. 5). The masked of the P_2 reaction in thermogram for the cortical sample could be related to the smaller amount of fluids in these samples than in cancellous samples.

P_3 peak appears overlaid on the low temperature tail of a high temperature process, P_4, whose maximum appears at around 410 K. The inset in Fig. 5 shows the P_4 peak without the water contribution, i.e. the subtraction of P_3 peak. This last peak (P_4) can be related both to the collagen/protein denaturation [27] and to the loss of the non-free water, the so called crystallisation water. Crystallisation water is used in compounds of proteins and/or collagen-apatite bonds [4, 29 – 31]. In addition, during a subsequent second heating run both cancellous and cortical samples do not show any thermal reaction.

The loss of weight ρ measured during heating for cancellous (b) and cortical (c) samples is shown in Fig. 6. A first stage up to around 380 K is shown for the two types of samples. This first decrease corresponds to the water release during heating and is similar in both cases. A water loss of around 7% below 400 K was estimated in reasonable agreement with the DSC results taking into account the accumulative procedure to determine the weight loss (see Section Measurement). Above 450 K the weight loss increases but both curves visibly split. This temperature range, where a stage

develops for the cortical sample, corresponds to the temperature of the P_4 endothermic reaction in the DSC curve, then it could be related to the collagen/protein denaturation and also to the loss of crystallisation water.

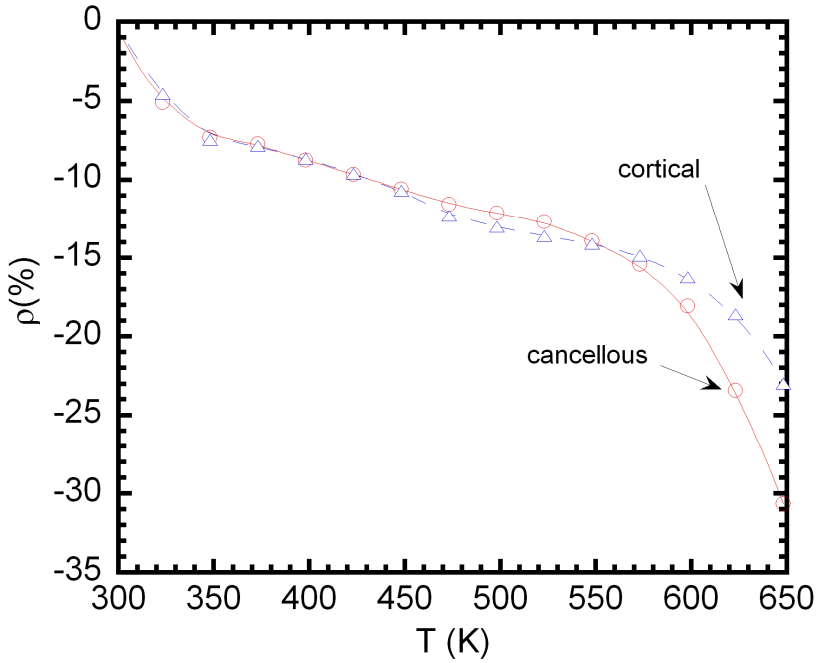

Figure 6. Weight loss (in percent), ρ, as a function of temperature for cancellous (b sample) and cortical (c sample) bones. Lines are guidelines for the eye.

The denaturation process at around 320 K (P_2 reaction in Fig. 5) lead to the increase of damping in the cancellous part due to the increase in mobility of the frictional micromechanisms (removal of elastic constrains) giving rise to the first increase of the frictional terms at around 320 K (see Fig. 2 to Fig. 4). In addition, the melting of fats plays the role of a plasticiser into the bone matrix leading also to the increase of damping values. Besides, the resonance frequency (Fig. 2(b) and Fig. 4(b)) increases above 320 K indicating that other physical mechanism is occurring overlapped to the denaturation and melting processes. The loss of water and fluids observed by DSC and TGA, Fig. 5 and Fig. 6, during the warming leads to the decrease in the viscous capacity of the frictional micromechanisms and then it increases the oscillating frequency and decreases the damping values for temperatures over 320 K. Therefore, the non thermally activated maximum in damping at around 320 K (see Fig. 3) is the result of the overlapping and competition of the two different physical and chemical processes taking place in the cancellous part: (i) An increase of damping related to both the denaturation of albumin and haemoglobin proteins and the melting of fats and (ii) A subsequent decrease in damping related the loss of water and fluids.

Concerning the damping peak at around 350K in (a) and (b) samples, the change in the morphological shape which leads to a compactness arrangement of the cancellous bone could be the mechanism responsible for promoting this peak. In fact Fig. 7(a) and Fig. 7(b) show the morphology of the cancellous bone prior and after heating to 410 K, respectively. The heated sample exhibits an arrangement more compact than the fresh one. This higher compactness in heat treated samples at temperatures above 350 K is promoted by the shrinkage of the cancellous part due to the denaturation of the proteins above 320 K and the massive loss of water and fluids [4, 23, 32, 33], as it was determined from DSC and TGA studies (see Fig. 5 and Fig. 6). During the shrinkage of the cancellous bone the preponderant mechanism is the decrease in the free space which leads to a more constrained arrangement of the matrix leading to the increase in the oscillating frequency and to the decrease in the damping. However, the shrinkage process, promotes also a large modification of the matrix which could cause the appearance of new cracks and voids. It leads to the increase in

damping giving rise to the peak shaped response at around 350 K overlaid to the whole decreasing trend of damping curve (see Fig. 4).

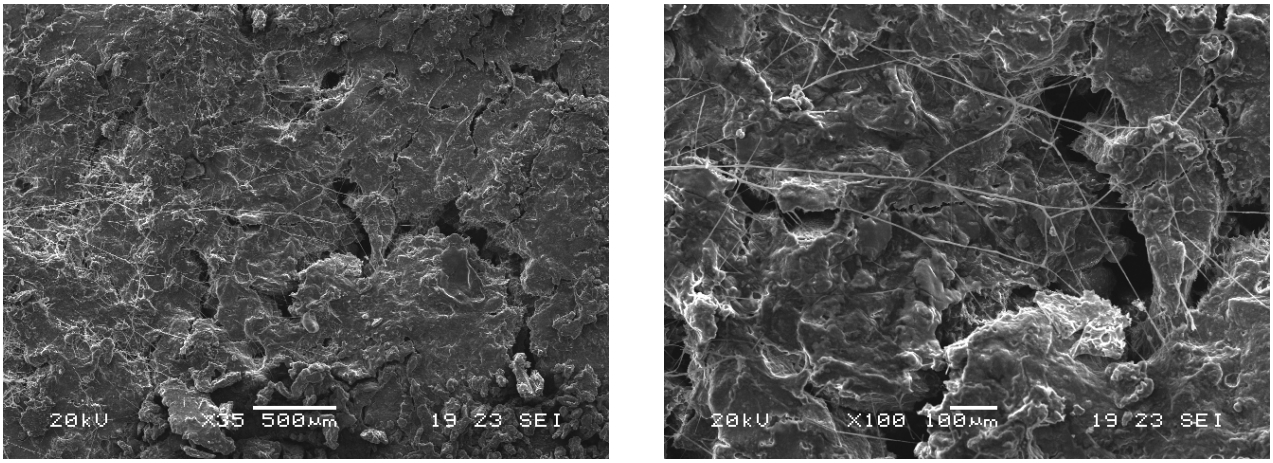

Figure 7(a). SEM micrographs for a b-type sample before heating.

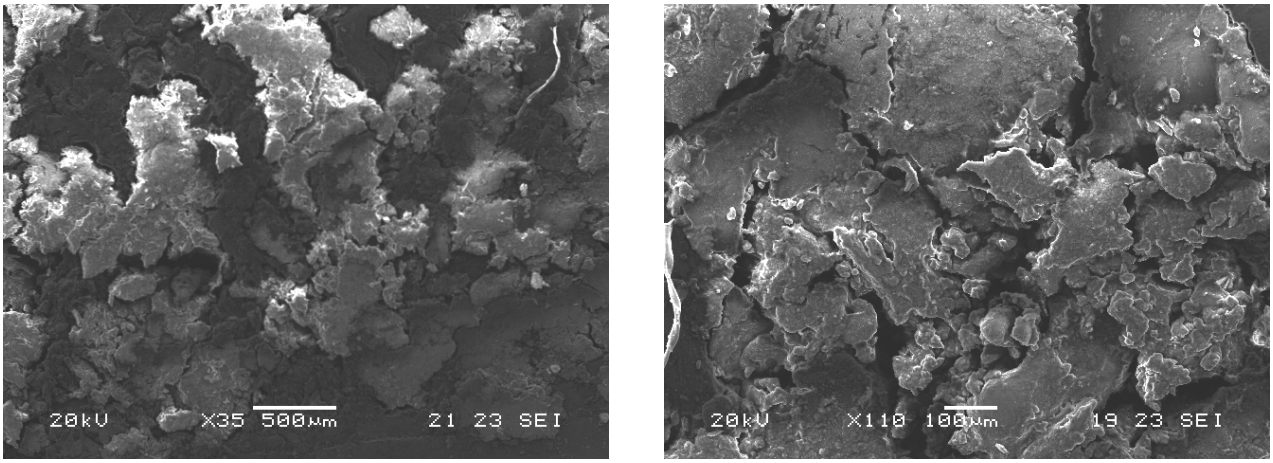

Figure 7(b). SEM micrographs for a b-type sample after heating to 410 K.

In contrast, in cortical bone the damping spectrum exhibits a wide damping peak between around 300 K - 400 K. The maximum damping value is reached at around 320K, so this dissipative mechanism can be related to the overlap of the processes (i) and (ii) which occur in the cancellous part within this temperature range. The high sensitivity of MS test allows us to confirm the appearance of the denaturation of albumin and haemoglobin, which is weakly suggested from DSC in Fig. 5. In addition, the continuous loss of water and fluids during heating give rise to both the decrease in damping and the increase in frequency (see Fig. 4). Moreover, as clear changes in cortical type samples after the warming up to 410 K could not be detected through SEM examinations, the shrinkage of the mesostructure in cortical bones can be neglected during the loss of water and fluids, then the damping peak at around 350 K is absent. It is in agreement with the smaller frequency increase during heating than in cancellous samples, see Fig. 4(b).

On the other hand, a hump in the damping spectrum corresponding to cortical samples develops from around 380 K up to 410 K, which is absent in cancellous ones, see Fig. 4(a). The appearance of this hump could be related to the development of another overlaid relaxation process. Indeed, as it was shown by means of DSC studies, the cortical samples exhibit the P_4 endothermic reaction related to the collagen/protein denaturation and to the loss of crystallisation water, which ranges from around 370 K up to 500 K, see inset in Fig. 5. Consequently, the appearance of the relaxation process from around 380 K up to 410K in cortical samples could be related to the collagen/protein denaturation and to the loss of crystallisation water. This mechanism controlling damping behaviour in cortical samples results in agreement with the almost flat behaviour exhibited by the damping

values for cancellous samples and the non appearance of P_4 reaction in DSC studies. However, more effort must be done in the study of the physical and chemical mechanisms involved in the connection of P_4 reaction and its influence on damping behaviour in bones at temperatures close to 400 K.

Conclusions

The physical-chemical mechanisms that control the wide damping maximum in bones samples, between around 280 K and 420 K in the MS tests; have been determined by coupling DSC, TGA and SEM studies. This maximum is the result of the overlapping of different processes taking place at different temperatures in the cancellous and cortical parts.

A damping peak at around 320 K develops both in cancellous and cortical bone. It is controlled by the overlap of the following processes: (i) the denaturation of albumin and haemoglobin proteins and also the melting of fats, (ii) the loss of water during heating at temperatures over room temperature.

A damping peak at 350 K appears in cancellous bone only and is controlled by the shrinkages of the mesostructure of bone owing to the loss of water.

The collagen/protein denaturation and the loss of crystallisation water, in cortical bones, give rise to another relaxation process from around 390 K up to 410 K. More effort must be done in the study of the physical and chemical processes involved in this relaxation process.

Acknowledgements

This work was partially supported by the CONICET-PIP No. 2098 and the PID-UNR ING 288 and ING 290 (2010–2013).

References

[1] A. Ascenzi, A. Benvenuti, Orientation of collagen fibers at the boundary between two successive osteonic lamellae and its mechanical interpretation, J. of Biomech. 19 (1986) 455 – 463.
[2] V. Cane, G. Marotti, G. Volpi, D. Zaffe, S. Palazzini, F. Remaggi, M.A. Muglia, Size and density of osteocyte lacunae in different regions of long bones, Calcified Tissue Int. 34 (1982) 558 – 563.
[3] E.B. Garner, R. Lakes, T. Lee, C. Swan, R. Brand, Viscoelastic dissipation in compact bone: Implications for stress-induced fluid flow in bone, J. Biomech. Eng. 122 (2000) 166 – 172.
[4] J.F. Mano, Viscoelastic properties of bone: Mechanical spectroscopy studies on a chicken model, Mat. Sci. Eng. C, 25 (2005) 145 – 152.
[5] R. Schaller, S. Barrault, Ph. Zysset, Mechanical spectroscopy of bovine compact bone, Mat. Sci. Eng. A, 370 (2004) 569 – 574.
[6] M.F. Ashby, L.J. Gibson, Cellular solids structure and properties. Cambridge University Press, Cambridge, 1997.
[7] J.S. Yerramshetty, O. Akkus, The associations between mineral crystallinity and the mechanical properties of human cortical bone, Bone, 42 (2008) 476 – 482.
[8] R. Schaller, G. Fantozzi, G. Gremaud, Mechanical Spectroscopy, Trans. Tech. Publications Ltd., Switzerland, 2001.
[9] B.J. Lazan, Damping of materials and members in structural mechanics, Pergamon, London, 1968.
[10] T. Wang, Z. Feng, Dynamic mechanical properties of cortical bone: The effect of mineral content, Mater. Lett. 59 (2005) 2277 – 2280.

[11] N.W. Tschoegel, The phenomenological theory of linear viscoelastic behaivour, Springer-Verlag, Berlin, 1989.
[12] O.A. Lambri, A Review on the problem of measuring non-linear damping and the obtainment of intrinsic damping, in: Walgraef, D.; Martínez-Mardones, J. and Wörner, C. H. (Eds.), Materials Instabilities, World Scientific Publishing Co. Pte. Ltd., 2000, pp. 249 – 280.
[13] L.M. Salvatierra, O.A. Lambri, C.L. Matteo, P.A. Sorichetti, C.A. Celauro, R.E. Bolmaro, Growing of crystalline zones in EPDM irradiated with a low neutron flux, Nucl. Instrum. Meth. B, 225 (2004) 297 – 304.
[14] O.A. Lambri, L.M. Salvatierra, F.A. Sánchez, C.L. Matteo, P.A. Sorichetti, C.A. Celauro, Crystal growth in EPDM by chemi-crystallisation as a function of the neutron irradiation dose and flux level, Nucl. Instrum. Meth. B, 237 (2005) 550 – 562.
[15] O.A. Lambri, J.A. García, W. Riehemann, J.A. Cano, G.I. Zelada-Lambri, F. Plazaola, Dislocation movement in WE43 magnesium alloy during recovery and recrystallisation, Mater. T. JIM. 52 (2011) 1016 – 1025.
[16] O.A. Lambri, W. Riehemann, Z. Trojanová, Mechanical spectroscopy of commercial AZ91 magnesium alloy, Scripta Mater. 45 (2001) 1365 – 1371.
[17] O.A. Lambri, G.I. Zelada-Lambri, G.J. Cuello, P.B. Bozzano, J.A. García, Study of the temperature evolution of defect agglomerates in neutron irradiated molybdenum single crystals, J. Nucl. Mater. 385 (2009) 552 – 558.
[18] T. Mura, Micromechanics of defects in solids, Martinus Nijhoff Publishers, New York, 1987.
[19] O.A. Lambri, W. Riehemann, Damping due to incoherent precipitates in commercial QE22 magnesium alloy, Scripta Mater. 52 (2005) 93 – 97.
[20] G.I. Zelada-Lambri, O.A. Lambri, G.H. Rubiolo, Amplitude dependent damping in austenitic stainless steels 316H and 304H. Its relation with the microstructure, J. Nucl. Mater. 273 (1999) 248 – 256.
[21] R.R. Mocellini, O.A. Lambri, C.L. Matteo, J.A. García, G.I. Zelada-Lambri, P.A. Sorichetti, F. Plazaola, A. Rodríguez-Garraza, F.A. Sánchez, Elastic misfit in two-phase polymer, Polymer, 50 (2009) 4696 – 4705.
[22] O.A. Lambri, F. Plazaola, E. Axpe, R.R. Mocellini, G.I. Zelada-Lambri, J.A. García, C.L. Matteo, P.A. Sorichetti, Modification of the mesoscopic structure in neutron irradiated EPDM viewed through positron annihilation spectroscopy and dynamic mechanical analysis, Nucl. Instrum. Meth. B, 269 (2011) 336 – 344.
[23] M.L. Lambri, J.I. Pérez-Landazábal, V. Recarte, F. Tarditti, O.A. Lambri, Effect of the mesostructure on the mechanical dynamical behaviour in cancellous bones, Acta Microscópica, 22 (2013) 26 – 31.
[24] A.S. Nowick, B.S. Berry, Anelastic Relaxation in Crystalline Solids, Academic Press, New York, 1972.
[25] O.A. Lambri, A.L. Peñaloza, A.V. Morón Alcain, M.L. Ortiz, F.C. Lucca, Mecahnical dynamical spectroscopy in Cu-Li alloys produced by electrodeposition, Mat. Sci. Eng. A, 212 (1996) 108 – 118.
[26] I.M. Ward, Mechanical properties of solid polymers, John Wiley & Sons, New York, 1990.
[27] V. Uskokovic, N. Ignjatovic, N. Petranovic, Synthesis and characterization of hydroxyapatite-collagen biocomposite materials, Mater. Sci. Forum, 413 (2003) 269 – 274.
[28] J. Benedito, J.A. Carcel, C. Rosello, A. Mulet, Composition assessment of raw meat mixtures using ultrasonics, Meat Sci. 57 (2001) 365 – 370.
[29] J.A. Babor, J. Ibarz, Modern general chemistry, Marín, Barcelona, 1965.
[30] B.D. Hames, N.M. Hooper, Instant notes biochemistry, Second edition, BIOS Scientific Publishers, England, 2000.

[31] J. Yamashita, B.R. Furman, H.R Rawls, X. Wang, C.M. Agrawal, The use of dynamic analysis to assess the viscoelastic properties of human cortical bone, J. Biomed. Mater. Res. 58 (2001) 47 – 53.
[32] Y. Dekhtyar, A. Gamza, A. Tatarinov, H. Jansons, Electron and mechanical properties of bone during heating, evaluated by exoelectron emission and ultrasound, Biomaterials 16 (1995) 861 – 863.
[33] K.O. Honikel, Reference methods for the assessment of physical characteristics of meat, Meat Sci. 49 (1998) 447 – 457.

Journal of Biomimetics, Biomaterials & Tissue Engineering Vol. 19
10.4028/www.scientific.net/JBBTE.19

Damping Micromechanisms for Bones above Room Temperature
10.4028/www.scientific.net/JBBTE.19.87